
Accounting for stochasticity in demographic compensation along the elevational range of an alpine plant

Andrello Marco ^{1,*}, De Villemereuil Pierre ², Carboni Marta ³, Busson Delphine ⁴, Fortin Marie-Josée ⁵, Gaggiotti Oscar E ⁶, Till-Bottraud Irene ⁷

¹ MARBEC, Univ Montpellier, CNRS, IFREMER, IRD, Sète, France

² Institut de Systématique, Évolution, Biodiversité (ISYEB), École Pratique des Hautes Études PSL, MNHN, CNRS, Sorbonne Université, Université des Antilles, Paris, France

³ Dipartimento di Scienze, Università Degli Studi di Roma Tre, viale Marconi 446, 00146 Roma, Italy

⁴ Laboratoire d'Ecologie Alpine (LECA), Université Grenoble Alpes, F-38000 Grenoble, France; CNRS, LECA, F-38000 Grenoble, France

⁵ Department of Ecology and Evolutionary Biology, University of Toronto, Toronto, M5S 3B2, Canada

⁶ Scottish Oceans Institute, University of St Andrews, Fife, KY16 8LB, United Kingdom.

⁷ Université Clermont Auvergne, CNRS, GEOLAB, F-63000 Clermont-Ferrand, France

* Corresponding author : Marco Andrello, email address : marco.andrello@ird.fr

Abstract :

Demographic compensation arises when vital rates change in opposite directions across populations, buffering the variation in population growth rates, and is a mechanism often invoked to explain the stability of species geographic ranges. However, studies on demographic compensation have disregarded the effects of temporal variation in vital rates and their temporal correlations, despite theoretical evidence that stochastic dynamics can affect population persistence in temporally varying environments. We carried out a seven-year-long demographic study on the perennial plant *Arabis alpina* across six populations encompassing most of its elevational range. We discovered demographic compensation in the form of negative correlations between the means of plant vital rates, but also between their temporal coefficients of variation, correlations and elasticities. Even if their contribution to demographic compensation was small, this highlights a previously overlooked, but potentially important, role of stochastic processes in stabilizing population dynamics at range margins.

Keywords : *Arabis alpina*, Brassicaceae, elasticity, elevation, population dynamics, stochasticity

50 INTRODUCTION

51 One of the processes shaping population performance across species ranges is demographic
52 compensation between different vital rates, such as recruitment, survival, growth and reproduction
53 (Doak & Morris 2010; Villellas *et al.* 2015). Demographic compensation arises when different vital rates
54 change in opposite directions across populations in response to environmental gradients, and has been
55 proposed as a mechanism increasing the range of environments over which a species can occur and to
56 explain the apparent stability of species range margins despite strong temporal environmental changes
57 (Doak & Morris 2010; Sheth & Angert 2018). So far, the paradigm of demographic compensation has
58 considered spatial differences in vital rates averaged over years, while disregarding the role of spatial
59 differences in temporal variation of vital rates (Villellas *et al.* 2015). However, because temporal
60 variation in vital rates can be higher in some parts of a species geographical range (for example, at range
61 margins; Angert 2009; Pironon *et al.* 2017), population growth rates might vary across species ranges not
62 only because of spatial variation in mean vital rates, but also in their temporal variability.

63 Population dynamics in temporally varying environments have received much attention in ecology and
64 conservation (Tuljapurkar 1990; Lande *et al.* 2003). Theory predicts that temporal variability should
65 decrease population growth rates in both structured and unstructured populations (Lewontin & Cohen
66 1969; Tuljapurkar 1990) and empirical studies support these predictions (Morris *et al.* 2008). In addition,
67 positive temporal covariations between vital rates can potentially amplify the effects of environmental
68 stochasticity on population dynamics, while negative temporal covariation can buffer it (Doak *et al.*
69 2005; Jongejans *et al.* 2010; Compagnoni *et al.* 2016). For example, positive covariances between
70 reproduction and survival rates tend to magnify the effect of variability and lead to lower population
71 growth rates than in the case of zero or negative covariances (Jongejans *et al.* 2010). Finally, the
72 elasticities of population growth rates, which measure the change in population growth rate caused by a

73 change in demographic parameters, determine the ultimate effects of temporal variation and vital rate
74 correlations on the population growth rate (Caswell 2001; Tuljapurkar *et al.* 2003). The interplay of these
75 factors is perhaps best summarized by writing the stochastic population growth rate $\log\lambda_s$ using the
76 small-noise approximation, as a function of the intrinsic growth rate $\log\lambda_d$ (calculated using the temporal
77 means of vital rates) minus a product containing temporal coefficients of variation of vital rates (CV_k and
78 CV_l), correlations between vital rates (ρ_{kl}) and vital rate elasticities (e_k and e_l) (Tuljapurkar 1990):

$$79 \log\lambda_s \approx \log\lambda_d - \frac{1}{2} \sum_{k,l} CV_k CV_l \rho_{k,l} e_k e_l \quad (\text{eq. 1})$$

80 Thus, a full picture of how population dynamics change across populations requires quantifying the
81 differences in how mean vital rates, their temporal variation, their correlations and the elasticities
82 change between populations. Such differences between populations can ultimately determine processes
83 of demographic compensation and can thus inform on the stability and dynamics of species ranges (Doak
84 & Morris 2010; Villellas *et al.* 2013).

85 Elevational ranges offer a unique opportunity to study range-wide variation in vital rates and population
86 dynamics at a tractable spatial scale. For plants, elevational ranges have been associated with large
87 differences in life-histories (Laiolo & Obeso 2017). Species living at lower elevations have often larger
88 sizes, higher mortality rates, shorter lifespans and higher fecundities, while species living at higher
89 elevations have smaller sizes, lower mortality rates, longer life spans and reduced flowering rates (Nobis
90 & Schweingruber 2013; Laiolo & Obeso 2017). These life-history patterns have been related to
91 predictions from the r-K selection theory (Pianka 1970), the metabolic theory of ecology (Brown *et al.*
92 2004) and the acquisitive and stress-tolerant strategies of functional ecology (Read *et al.* 2014). While
93 many studies have uncovered elevational patterns in plant life-histories across species, studies on
94 population dynamics are less common, and patterns of variation in plant population growth rates along
95 elevational gradients are less clear. Indeed, the few studies focusing on dynamics of herbaceous plant

96 populations on elevational gradients report increasing (Miller *et al.* 2009; Giménez-Benavides *et al.*
97 2011), decreasing (Kim & Donohue 2011; Pena-Gomez & Bustamante 2012) and stable (García-Camacho
98 *et al.* 2012) patterns of population growth rates with elevation.

99 Here, we aimed at testing whether spatial patterns in temporal variation, temporal correlations and
100 elasticities could be involved in demographic compensation beyond the spatial variation of average vital
101 rates, thereby contributing to the stabilization of species elevational ranges. To this end, we carried out a
102 population dynamics study on *Arabis alpina* (Brassicaceae), a broadly distributed arctic-alpine perennial
103 herb, across most of its elevational range in the European Alps. Specifically, our goals were twofold. First,
104 we aimed at quantifying the spatial variation of four different descriptors of stochastic population
105 dynamics (means, coefficients of variation, correlations and elasticities of plant vital rates) across an
106 elevational gradient. Second, we aimed at quantifying the contributions of each of the four descriptors
107 to the stochastic population growth rate and test for demographic compensation between different
108 descriptors.

109 MATERIALS AND METHODS

110 Model species

111 *Arabis alpina* (L., Brassicaceae) is emerging as a new model organism in plant ecology and evolutionary
112 biology (e.g. Wang *et al.* 2009; de Villemereuil *et al.* 2018) due to its perennial life-cycle and wide
113 elevational distribution. It occurs primarily in the subalpine and alpine belts, predominantly in open,
114 unstable, moist sites with low vegetation cover such as glacier forelands, scree slopes, rock ledges,
115 footpaths and small streams, often in association with calcareous soil (Lauber *et al.* 2018). Seedlings
116 germinate and establish throughout the growing season, plants flower for a few weeks and produce
117 fruits (siliques), and flowering stems eventually wilt and die (Wang *et al.* 2009). Seeds can persist in the
118 soil and form a permanent seed bank (Diemer & Prock 1993; Philipp *et al.* 2018).

119 Data collection

120 This study was conducted in six sites spanning most of the elevational range of *A. alpina* in the European
121 Alps using permanent plots (**Table 1, Figure S1**), which were visited once a year after flowering between
122 2008 and 2014 to record the number of stems and siliques of each individual (See **Appendix S1.1** in
123 **Supporting Information**). *In-situ* germination tests were not successful, so germination rates could not
124 be estimated locally and seed bank dynamics was disregarded in the matrix population model, but we
125 conducted a sensitivity analysis to assess the effects of uncertainty in seed germination on the results
126 (Nguyen *et al.* 2019; **Appendix S1.5, S2.2**).

127 Microclimatic conditions, soil chemistry and species composition of the vegetation were measured in
128 each plot to model plant vital rates in function of environmental conditions. Temperature data loggers
129 (iButton® Hygrochron, Maxim Integrated™) provided estimates of summer daily mean temperature
130 (T_{mean}) and daily temperature range (T_{range} ; **Table 1**). Missing records (due to malfunctioning of the data-
131 loggers) were imputed using data from nearby weather stations, resulting in ten resampled datasets

132 **(Appendix S1.2)**. Soil acidity (pH), total soil carbon and nitrogen content were determined following
133 standard methods (Schinner *et al.* 1996). Abundance-dominance (Braun-Blanquet) lists of plant species
134 were used to calculate abundance weighted means for vegetative height and specific leaf area (SLA),
135 using values from the ANDROSACE (Thuiller *et al.* 2014) and the TRY (Kattge *et al.* 2011) databases. After
136 performing a principal component analysis on the three soil variables and the two vegetation variables
137 **(Appendix 2.1, Figure S3, S4)**, we retained the first two axes to predict plant vital rates: *SoilVeg₁*
138 (explaining 52% of the variance), positively related to acidic soils with high C and N content, and *SoilVeg₂*
139 (explaining 29% of the variance), summarizing variation from slow-growing short vegetation to fast-
140 growing tall vegetation.

141 **Analysis**

142 We used a five-step approach to test how four *descriptors* (μ : means; *CV*: coefficients of variation; *e*:
143 elasticities; ρ : temporal correlations) of seven *life-cycle components* (*S*: survival; *G*⁻: retrogressive growth;
144 *G*⁻: stasis; *G*⁺: progressive growth; *F*₀: reproduction; *F*₁: fecundity; *F*₂: recruit size) contribute to
145 demographic compensation across the elevational range of *A. alpina*. First, we constructed matrix
146 population models for each site and year using statistical models predicting plant vital rates from
147 environmental variables (Step 1). Second, we used the matrix models to calculate the seven life-cycle
148 components, stochastic population growth rate $\log\lambda_s$ and elasticities of $\log\lambda_s$ (Step 2). Third, we tested
149 for significant relationships between elevation and population dynamics variables (Step 3). Fourth, we
150 performed a stochastic life-table response experiment (SLTRE) in order to decompose the differences in
151 $\log\lambda_s$ between sites into contributions C_l^k of each life-cycle component *l* and each descriptor *k* (Step 4).
152 Finally, we assessed demographic compensation by testing for negative and positive correlations
153 between the SLTRE contributions C_l^k (Step 5).

154 *Step 1. Prediction of plant vital rates*

155 The plant vital rates used to construct the matrix population models were survival (whether the plant
156 survives to $t + 1$ or not), size (the size of the plant at time $t + 1$, conditional on survival), reproduction
157 (whether the plant bears siliques or not at time t), reproductive output (the number of siliques of the
158 plant at time t , conditional on reproduction) and recruit size. Plant vital rates were predicted using
159 generalized linear mixed models (GLMMs; Zuur *et al.* 2009) as a function of plant size at time t (except
160 for recruit size that, by definition, did not exist at time t), T_{mean} , T_{range} , $SoilVeg_1$ and $SoilVeg_2$ treated as
161 fixed effects; plant size at time t and T_{mean} were also included as quadratic terms. Site, year nested within
162 site and plot nested within site were included as random effects on the intercept and the slopes when
163 significant. The error structure of the models was Gaussian (for \log_{10} -transformed reproductive output),
164 Bernoulli (for survival and reproduction), or negative binomial (for growth and recruit size). We
165 accounted for uncertainty in the data using a total 2000 bootstrap samples over the ten imputed climatic
166 datasets. For each bootstrap sample, we fitted the $2^7=128$ models corresponding to the combinations of
167 the predictors, sampled one of them according to its Akaike weight (Burnham & Anderson 2002),
168 obtained site- and year-specific predictions of vital rates (by setting predictors to their mean values over
169 the plots of each site and year) and constructed matrix models to perform all the subsequent population
170 dynamics analyses. Means and 95% confidence intervals for the reported results were calculated from
171 the 2000 predicted values using the percentile method. All analyses were run in R 3.6.0 with packages
172 *lme4* 1.1-21 and *MuMIn* 1.43.6 (Bartoń 2009; Bates et al. 2015; **Appendix S1.3**).

173 *Step 2. Population dynamics analyses*

174 We defined a matrix population model (Caswell 2001) with 50 size classes of one-stem each, which
175 covered the range of variation in plant sizes observed in the field. The projection matrix **A** was the sum
176 of the transition matrix **P** = [p_{ij}] and the fecundity matrix **F** = [f_{ij}], which were constructed using the
177 predicted vital rates obtained in Step 1:

178 $p_{ij} = s_j g_{ij}$

179 $f_{ij} = \varepsilon F_{0,j} F_{1,j} F_{2,i}$ (eq. 2)

180 where j is plant size in year t ; i is plant size in year $t+1$; s_j (survival) g_{ij} (growth), $F_{0,j}$ (reproduction), $F_{1,j}$
181 (reproductive output) and $F_{2,i}$ (recruit size) are the predicted vital rates. $\varepsilon = 0.02$ is a seedling
182 establishment coefficient converting the number of fruits in one year to the number of seedling in the
183 following year, and was set equal to the median value of the ratio of the observed number of seedlings
184 to the number of fruits in the previous year over all plots and sites.

185 Life-cycle components for each site and year were calculated as averages of the predicted vital rates over
186 size classes weighted by the stable stage distribution vector (Salguero-Gómez *et al.* 2016). Specifically, S ,
187 F_0 and F_1 were calculated as weighted averages of the s_j 's, $F_{0,j}$'s and $F_{1,j}$'s (eq. 2), respectively. G^-
188 represents transitions from larger to smaller size classes and was calculated as the weighted average of
189 all the g_{ij} 's for which $i < j$. Similarly, G^- (representing individuals not changing in size) and G^+ (representing
190 transitions to larger size classes) were calculated as weighted averages of all the g_{ij} 's for which $i = j$ and i
191 $> j$, respectively. F_2 was calculated as the mean recruit size distribution $F_{2,i}$.

192 For each site, we calculated the temporal means and coefficients of variation of each life-cycle
193 component and temporal correlations between pairs of life-cycle components (Pearson's correlation)
194 over years. The stochastic population growth rate $\log \lambda_s$ was calculated via the simulation method by
195 randomly sampling one of the year-specific matrix at each iteration (Caswell 2001, p. 396). We then
196 calculated the elasticities of $\log \lambda_s$ to changes in the mean and standard deviation of the stage-specific
197 vital rates (Tuljapurkar *et al.* 2003). We obtained the elasticities to the mean and standard deviation of
198 life-cycle components by summing the elasticities of the respective vital rates (Franco & Silvertown 2004;
199 **Appendix S1.4**).

200 *Step 3. Elevational patterns*

201 We used linear regressions to test for significant relationships between elevation and population
202 dynamics variables: mean life-cycle components, coefficients of variation of life-cycle components,
203 temporal correlations between life-cycle components, $\log\lambda_s$ and elasticities.

204 *Step 4. Stochastic life-table response experiment (SLTRE)*

205 We calculated the differences in $\log\lambda_s$ ($\Delta \log\lambda_s^{(m)}$) between each site m and a common reference site
206 defined by the means of vital rates over sites. The $\Delta \log\lambda_s^{(m)}$ were decomposed into the contributions
207 $C_{x_i, x_j}^{k, (m)}$ of differences of each descriptor k (mean μ ; coefficient of variation CV ; temporal correlations ρ ;
208 elasticities e) of stage-specific vital rates x_i (survival s_j , growth g_{ij} , reproduction F_{0j} , reproductive output
209 F_{1j} and recruit size F_{2i}) according to the SLTRE of Davison *et al.* (2013; **Appendix S1.6**):

$$210 \Delta \log\lambda_s^{(m)} \approx \sum_i C_{x_i}^{\mu, (m)} + \sum_{i,j} C_{x_i, x_j}^{CV, (m)} + \sum_{i,j} C_{x_i, x_j}^{\rho, (m)} + \sum_{i,j} C_{x_i, x_j}^{e, (m)} \quad (\text{eq. 3})$$

211 From this decomposition, we derived the *net contributions* C_l^k of each life-cycle component l and each
212 descriptor k by summing the $C_{x_i, x_j}^{k, (m)}$ according to the definition of life-cycle components given above. The
213 *total effect* C_l of each life-cycle component was calculated by summing the absolute values of its
214 contributions over the four descriptors, $C_l = \sum_k |C_l^k|$. Similarly, the *total effect* C^k of each descriptor was
215 calculated by summing the absolute values of its contributions over life-cycle components, $C^k = \sum_l |C_l^k|$.
216 Finally, we used linear regressions to test for significant relationships between elevation and the net
217 contributions C_l^k .

218 *Step 5. Demographic compensation*

219 To test for demographic compensation and its effectiveness in reducing the spatial variation in
220 population growth rates, we extended the approach of Villellas *et al.* (2015) to all descriptors of life-cycle
221 components. We tested for demographic compensation by testing for negative and positive Spearman

222 correlations between the net contributions C_l^k . The occurrence of a significantly higher number of
223 significant negative correlations (or a significantly lower number of significant positive correlations) than
224 expected by chance is indicative of demographic compensation and was tested by permuting 1000 times
225 the C_l^k over sites. This permutation test assesses only the occurrence of demographic compensation but
226 not its effectiveness in reducing the variance in $\log\lambda_s$ among sites, $\sigma_{\log\lambda_s}^2$. We then performed additional
227 randomization tests where we calculated $\sigma_{\log\lambda_s}^2$ following the permutation of each net contribution C_l^k
228 at a time (thus 28 parameters). Higher values of $\sigma_{\log\lambda_s}^2$ in the randomization indicated that the focal
229 parameter reduced $\sigma_{\log\lambda_s}^2$ through its negative correlations; conversely, lower values for $\sigma_{\log\lambda_s}^2$ indicated
230 that the focal parameter increased $\sigma_{\log\lambda_s}^2$ through its positive correlations. Finally, we ran a
231 randomization test where we permuted only those C_l^k that reduced $\sigma_{\log\lambda_s}^2$: this randomization
232 procedure eliminates as much as possible the negative correlations while preserving the important
233 positive correlations and indicates the overall effectiveness of demographic compensation (Villellas *et al.*
234 2015).

235 RESULTS

236 Step 1. Prediction of plant vital rates

237 Plant size had significant effects on all vital rates (**Table 2**). Size and reproductive output were positively
238 affected by *SoilVeg₂*, which was itself positively related to vegetative height and SLA of the surrounding
239 vegetation (**Appendix S2.1**). Survival was positively affected by mean temperature squared (T_{mean}^2),
240 while recruit size was negatively affected by temperature range (T_{range}). However, the models for survival
241 and recruit size had remarkably low explanatory power (marginal $R^2 = 0.07$ and 0.04 , respectively). All
242 vital rates showed considerable spatial and temporal variation that was unexplained by our
243 environmental variables (conditional R^2 larger than marginal R^2).

244 Step 2. Population dynamics analyses

245 On average, survival probability was $S = 0.5$ (except in GAL where $S = 0.75$), progressive growth (G^+) was
246 larger than retrogressive growth (G^-) and stasis ($G^=$), reproduction was $F_0 = 0.5$, reproductive output was
247 $F_1 = 12$ siliques and recruit size was $F_2 = 1.5$ stems (**Figure 1 and S5**). Coefficients of variations (CV) were
248 mostly comprised between 0.1 and 0.6 across all life-cycle components. Over all sites and pairs of life-
249 cycle components, we observed 21 (17%) significant negative temporal correlations and 21 (17%)
250 significant positive temporal correlations (**Figure S6**).

251 The stochastic population growth rate $\log\lambda_s$ was negative in all sites (**Table 1**). One site (GAL) had higher
252 $\log\lambda_s$ than the other sites. The largest elasticities of $\log\lambda_s$ to the temporal means of life-cycle components
253 were associated with S , while the elasticities to G^+ were the second-largest (**Figure 1**). The elasticities of
254 $\log\lambda_s$ to the standard deviation of life-cycle components were largest and negative for S , intermediate for
255 G^+ and F_1 , and smallest for G^- , $G^=$, F_0 and F_2 .

256 **Step 3. Elevational patterns**

257 Mean survival (S), retrogressive growth (G^-) and stasis ($G^=$) increased significantly with elevation (**Figure**
258 **1**), while mean progressive growth (G^+), reproductive output (F_1) and recruit size (F_2) decreased
259 significantly with elevation. The CV of S, G^- and $G^=$ decreased significantly with elevation.

260 While the elasticities to mean S did not change with elevation, the elasticities to mean G^+ significantly
261 decreased with elevation. The elasticities to the means of the other life-cycle components were much
262 smaller and showed significant positive (G^- and $G^=$) or negative (F_0 , F_1 and F_2) relationships with elevation.
263 The elasticities to the standard deviation of life-cycle components did not change significantly with
264 elevation, nor did the temporal correlations between life-cycle components.

265 The stochastic growth rate $\log\lambda_s$ did not change significantly with elevation (**Figure S7**).

266 **Step 4. Stochastic life-table response experiment (SLTRE)**

267 The SLTRE showed that all four descriptors of life-cycle components (means, coefficients of variation,
268 temporal correlations and elasticities) contributed to differences in $\log\lambda_s$ between sites (**Figure 2**). Means
269 had the largest total effects in all sites, but the other descriptors were not negligible and could account
270 for up to 50% of the difference in the stochastic growth rate (**Figure 2a**): the largest effects were due to
271 coefficients of variation, while elasticities and correlations had smaller effects. When looking at the total
272 effects of each life-cycle component (**Figure 2b**), the largest ones were due to survival (S) and
273 progressive growth (G^+), while the other life-cycle components had smaller effects.

274 The net contributions of means and coefficients of variation of S (C_S^μ and C_S^{CV}) increased (became more
275 positive) with elevation, while the net contributions of mean G^+ ($C_{G^+}^\mu$) decreased (became more
276 negative) with elevation (**Figure S8**).

277 **Step 5. Demographic compensation**

278 There were 18 significant positive correlations and 22 significant negative correlations between the net
279 contributions of life-cycle components across sites. This constitutes substantial evidence for the
280 existence of demographic compensation according to the criterion proposed by Villellas *et al.* (2015),
281 since the number of negative correlations was much higher than expected by chance (permutation test,
282 **Figure 3**).

283 The negative correlations involved all four descriptors of population dynamics. While the correlations
284 linking G^- , G^- and G^+ together are trivial as they emerge from the same vital process (growth), the other
285 correlations are ecologically meaningful (**Figure S9**). Among these, there were significant negative
286 correlations involving mean life-cycle components (S , G^+ , F_1 and F_2), their coefficients of variation (S),
287 temporal correlations (S , G^- and G^-) and elasticities (G^- and G^+). Significant negative correlations linked
288 together the same descriptor of different life-cycle component (e.g. mean S and mean F_1), different
289 descriptors of the same life-cycle component (e.g. mean G^+ and its elasticity) and different descriptors of
290 different life-cycle components (the CV of S and the mean of G^+ , F_1 and F_2).

291 The parameters contributing the most to demographic compensation were mean S , mean G^+ and mean
292 F_1 , as their permutation generally increased the variance of $\log\lambda_s$ between sites, $\sigma_{\log\lambda_s}^2$ (**Figure 4a-d**).

293 Conversely, the permutation of the CV of S led to smaller $\sigma_{\log\lambda_s}^2$, indicating that this parameter increases
294 the variance in $\log\lambda_s$ relative to what would be expected by chance; this was the result of the numerous
295 positive correlations involving the CV of S (**Figure 3**). The other parameters did not change $\sigma_{\log\lambda_s}^2$
296 considerably. Randomizing only the parameters that reduced the variance in $\log\lambda_s$ between sites
297 indicated that the observed $\sigma_{\log\lambda_s}^2$ was 59% of the median $\sigma_{\log\lambda_s}^2$ expected under the hypothesis of
298 minimal negative correlations, but not significantly smaller ($p = 0.17$; **Figure 4e**).

299 **DISCUSSION**

300 In this work, we studied variation in population dynamics of *A. alpina* across most of its elevational range
301 in the European Alps (2000m). Contrary to the expectation that peripheral populations have lower
302 demographic performance than central populations (Pironon *et al.* 2017), *A. alpina* showed surprisingly
303 little variation in population growth rates $\log\lambda_s$ across its full elevational range. Conversely, most life-
304 cycle components significantly varied with elevation. We showed that this pattern could be partly
305 explained by demographic compensation, *i.e.* negative correlations between the contributions of
306 different life-cycle components to spatial differences in $\log\lambda_s$. In particular, compensatory effects across
307 the elevational range did not arise only through opposite spatial patterns in mean vital rates, but also in
308 their temporal variation, elasticities and temporal correlations. This highlights a previously overlooked,
309 but potentially important, role of stochastic processes in offsetting mean changes in vital rates and
310 stabilizing population dynamics at range margins. We now discuss the origin, significance and
311 generalities of the patterns of demographic compensation observed in this study.

312 The origin of negative correlations between the different descriptors of life-cycle components should be
313 searched in their patterns of variation along the elevational gradient (**Figure 1**). First, mean vital rates
314 changed in opposite directions: survival (S) increased along the elevational gradient while reproductive
315 output (F_1) decreased, resulting in a negative correlation between C_S^μ and $C_{F_1}^e$ (**Figure S9**). However,
316 stochastic descriptors also contributed to demographic compensation along elevation. For example, the
317 decrease in mean progressive growth (G^+), by itself, should have resulted in lower population growth
318 rates $\log\lambda_s$ at higher elevations. However, the elasticity to mean G^+ also decreased with elevation and
319 counterbalanced the negative effects of lower G^+ , because smaller elasticities dampen the effects of
320 changes in life-cycle components on $\log\lambda_s$. The CV of survival also decreased with elevation, further
321 offsetting the negative effects of lower G^+ , since smaller CV have positive effects on $\log\lambda_s$. The resulting

322 negative correlations between the net contributions of these parameters to $\log\lambda_s$ (namely, between $C_{G^+}^\mu$
323 and $C_{G^+}^e$ and between $C_{G^+}^\mu$ and C_S^{CV}) partly explain why population growth rates did not change with
324 elevation despite marked elevational gradients in life-cycle components. Overall, the observed patterns
325 are in agreement with the known higher occurrences of smaller and longer lived species and individuals
326 at higher elevations (Nobis & Schweingruber 2013; Laiolo & Obeso 2017) and higher variability of survival
327 at lower elevations (Angert 2009).

328 Such elevational patterns could be due to opposite responses of vital rates to common environmental
329 drivers (Knops *et al.* 2007). The main environmental driver of variation in growth and reproductive
330 output was *SoilVeg₂*, which summarizes variation in specific leaf area (SLA) and vegetative height
331 (**Appendix S2.1**), meaning that *A. alpina* tends to grow larger and produce more fruits when the
332 surrounding vegetation is composed of tall plants with large SLA. This relationship could indicate a
333 response to high competitive pressure or a common effect of temperature, because SLA and vegetative
334 height in plants tend to increase with temperature and decrease with elevation (Moles *et al.* 2014; Read
335 *et al.* 2014; Rosbakh *et al.* 2015). In contrast, the environmental drivers of survival are not easy to
336 identify, because the statistical model linking plant survival probability to environmental variables had
337 very low explanatory power. These results seem corroborated by a common garden experiment using
338 the same six populations as this study, which found that temperature was significantly associated with
339 total fruit length (a measure of reproductive output) but not with survival (de Villemereuil *et al.* 2018).
340 Elevational patterns in survival, growth and reproductive output could also be driven by other
341 environmental factors not considered in our analysis, such as soil phosphorus content, diversity of root
342 microbiota or herbivore damage, all of which affect various traits of *A. alpina* across its range (Almario *et al.*
343 *et al.* 2017; Buckley *et al.* 2019). Negative correlations between life-cycle components could also be due to
344 energetic trade-offs and structural constraints (Williams *et al.* 2015). In *A. alpina*, higher rates of
345 flowering are associated with reduction of plant survival, because all stems wilt and die after setting

346 seeds, to the point that mutants for perpetual flowering show an annual life-cycle (Wang *et al.* 2009).
347 Slower rates of stem production and/or lower rates of flowering could thus increase the longevity of the
348 entire plant, resulting in negative correlations between growth, reproduction and survival.

349 Spatial patterns in elasticity are not very documented, but increasing elasticities to survival with
350 elevation could result from their positive correlation with longevity (Silvertown *et al.* 1993; Franco &
351 Silvertown 2004) and from the positive correlation between longevity and elevation (Nobis &
352 Schweingruber 2013). In contrast, decreasing elasticities to fecundity and growth with elevation, as
353 found in our study, could be expected given that these elasticities correlate with SLA (Adler *et al.* 2014)
354 and SLA is known to decrease with elevation (Read *et al.* 2014). However, within-species patterns of
355 elasticities are also influenced by the level of environmental disturbance (Oostermeijer *et al.* 1996;
356 Silvertown *et al.* 1996), which may not show consistent variation with elevation.

357 The correlations between life-cycle components involved all descriptors of population dynamics but their
358 effectiveness for reducing the variance in $\log\lambda_s$ ($\sigma_{\log\lambda_s}^2$) was higher in the case of mean life-cycle
359 components. The effectiveness of a single descriptor for reducing $\sigma_{\log\lambda_s}^2$ through demographic
360 compensation depends on the strength and number of its negative correlations relative to its positive
361 correlations (**Figure 3**) and its contribution to the differences in $\log\lambda_s$ between sites, $\Delta\log\lambda_s$ (**Figure 2**).
362 Only parameters making large contributions change $\sigma_{\log\lambda_s}^2$ through their correlations, decreasing it when
363 most of their correlations are strong and negative. Mean progressive growth was the most important
364 parameter for demographic compensation by offsetting variation in survival. Mean survival and mean
365 reproductive output were the second most important parameters, thanks to their large contributions to
366 $\Delta\log\lambda_s$ and the negative correlation between them. Conversely, temporal correlations and elasticities
367 showed many significant negative correlations but they were not as important for demographic
368 compensation because the net contributions to $\Delta\log\lambda_s$ were small, in line with what is observed in other

369 plant species (Jongejans *et al.* 2010; Compagnoni *et al.* 2016; Davison *et al.* 2019). Finally, the CV of
370 survival made relatively large contributions to $\Delta\log\lambda_s$, but showed too many positive correlations that led
371 to an increase of $\sigma_{\log\lambda_s}^2$ rather than a reduction.

372 Although our results are comparable to findings over multiple species in the deterministic case (Villellas
373 *et al.* 2015), our study is the first assessing demographic compensation in a stochastic framework.

374 Assessing whether the results obtained here are representative of other species will require additional
375 studies quantifying both the contributions of all descriptors of population dynamics to $\Delta\log\lambda_s$ and their
376 pairwise correlations. The first exercise has been done by Davison *et al.* (2019) on a set of 62 species,
377 showing that more than one quarter of contributions to $\Delta\log\lambda_s$ can be attributed to the effect of
378 coefficients of variations, elasticities and temporal correlations. However, the importance of these
379 descriptors of population dynamics for demographic compensation remains unknown, as it depends
380 critically on the relative number and strength of negative vs. positive correlations in which they are
381 involved.

382 Even with demographic compensation, the stochastic population growth rate was negative in all sites,
383 indicating that populations are projected to decline in size and eventually go extinct locally. However, *A.*
384 *alpina* could persist thanks to germination from its persistent seed bank and immigration from other
385 sites (Hastings & Botsford 2006). Its frequent occurrence in unstable sites suggests that populations
386 could show an extinction-recolonization dynamics typical of metapopulations (Ouborg & Eriksson 2004).
387 The inclusion of a seed bank led to higher, sometimes positive population growth rates and confirmed
388 the existence of demographic compensation (**Appendix S2.2**). The effects of immigration are more
389 difficult to study in absence of estimates of seed dispersal rates, but the strong spatial genetic structure
390 of the populations ($F_{ST} = 0.6$, de Villemereuil *et al.* 2018) suggests that dispersal rates might be low. The
391 patterns of demographic compensation revealed here could thus be different in models integrating
392 empirical estimates of seed dormancy and germination rates and extinction-recolonization dynamics,

393 potentially unmasking greater importance for coefficients of variation, elasticities and temporal
394 correlations.

395 So far, demographic compensation has been discussed mainly in terms of spatial variation in mean vital
396 rates (Doak & Morris 2010; Villellas *et al.* 2015; Sheth & Angert 2018). Our study is the first to highlight
397 that temporal variation, elasticities and temporal correlations can be involved in demographic
398 compensation, even if their effect was smaller than that of means. Nonetheless, temporal variation in
399 vital rates could become more important under future expected increasing frequencies of extreme
400 climatic events (Meehl & Tebaldi 2004; Schär *et al.* 2004), such as summer heatwaves and drought, that
401 can cause large temporal variation in vital rates (Smith 2011; Andrello *et al.* 2012). Assessing the
402 importance of all descriptors of population dynamics for demographic compensation could thus provide
403 a more complete understanding of the dynamics of elevational as well as geographical species ranges in
404 a context of global change.

405 **ACKNOWLEDGEMENTS**

406 We thank Serge Aubert, Rolland Douzet and Bénédicte Poncet for helping us find the populations,
407 Hannah Secher Frommel and Cindy Arnoldi for soil analyses, Anne Delestrade for providing the weather
408 station data, three anonymous reviewers whose comments helped us improve the manuscript and all
409 the people who helped us in the field (in particular Florian Alberto, Perrine Augrit, Anne-Lise Bartalucci,
410 Justine Bisson, Jérémy Camazzola, Loïc Chalmandrier, Julie Chauvin, Lucas Hemery, Elsa Jullien, Aymeric
411 Pilleux, Blaise Tymen and Stefan Willhoit). MA and PDV were funded by a PhD scholarship by the French
412 Ministry of Research. This research was partially conducted at the Jardin Alpin du Lautaret, a member of
413 the AnaEE network (Infrastructure for Analysis and Experimentation on Ecosystems), and has used plant
414 trait values from the TRY initiative and data base ([http:// www.try-db.org](http://www.try-db.org)), which is hosted, developed
415 and maintained by J. Kattge and G. Bonisch (Max Planck Institute for Biogeochemistry, Jena, Germany),
416 and currently supported by DIVERSITAS/Future Earth and the German Centre for Integrative Biodiversity
417 Research (iDiv) Halle-Jena-Leipzig.

418 **LITERATURE CITED**

- 419 Adler, P.B., Salguero-Gomez, R., Compagnoni, A., Hsu, J.S., Ray-Mukherjee, J., Mbeau-Ache, C., *et al.*
 420 (2014). Functional traits explain variation in plant life history strategies. *Proceedings of the*
 421 *National Academy of Sciences*, 111, 740–745.
- 422 Almario, J., Jeena, G., Wunder, J., Langen, G., Zuccaro, A., Coupland, G., *et al.* (2017). Root-associated
 423 fungal microbiota of nonmycorrhizal *Arabis alpina* and its contribution to plant phosphorus
 424 nutrition. *PNAS*, 114, E9403–E9412.
- 425 Andrello, M., Bizoux, J.-P., Barbet-Massin, M., Gaudeul, M., Nicolè, F. & Till-Bottraud, I. (2012). Effects of
 426 management regimes and extreme climatic events on plant population viability in *Eryngium*
 427 *alpinum*. *Biological Conservation*, 147, 99–106.
- 428 Angert, A.L. (2009). The niche, limits to species' distributions, and spatiotemporal variation in
 429 demography across the elevation ranges of two monkeyflowers. *Proceedings of the National*
 430 *Academy of Sciences*, 106, 19693–19698.
- 431 Bartoń, K. (2009). *MuMIn: multi-model inference*. R package. .
- 432 Bates, D., Maechler, M., Bolker, B. & Walker, S. (2015). Fitting Linear Mixed-Effects Models Using lme4.
 433 *Journal of Statistical Software*, 67, 1–48.
- 434 Brown, J.H., Gillooly, J.F., Allen, A.P., Savage, V.M. & West, G.B. (2004). Toward a metabolic theory of
 435 ecology. *Ecology*, 85, 1771–1789.
- 436 Buckley, J., Widmer, A., Mescher, M.C. & De Moraes, C.M. (2019). Variation in growth and defence traits
 437 among plant populations at different elevations: Implications for adaptation to climate change.
 438 *Journal of Ecology*, 107, 2478–2492.
- 439 Burnham, K.P. & Anderson, D.R. (2002). *Model Selection and Multimodel Inference: A Practical*
 440 *Information-Theoretic Approach*. 2nd edn. Springer-Verlag, New York.
- 441 Caswell, H. (2001). *Matrix population models. Construction, analysis and interpretation*. Sinauer,
 442 Massachusetts.
- 443 Compagnoni, A., Bibian, A.J., Ochocki, B.M., Rogers, H.S., Schultz, E.L., Sneek, M.E., *et al.* (2016). The
 444 effect of demographic correlations on the stochastic population dynamics of perennial plants.
 445 *Ecological Monographs*, 86, 480–494.
- 446 Davison, R., Nicolè, F., Jacquemyn, H. & Tuljapurkar, S. (2013). Contributions of Covariance: Decomposing
 447 the components of stochastic population growth in *Cypripedium calceolus*. *Am Nat*, 181.
- 448 Davison, R., Stadman, M. & Jongejans, E. (2019). Stochastic effects contribute to population fitness
 449 differences. *Ecological Modelling*, 408, 108760.
- 450 Diemer, M. & Prock, S. (1993). Estimates of Alpine Seed Bank Size in Two Central European and One
 451 Scandinavian Subarctic Plant Communities. *Arctic and Alpine Research*, 25, 194.
- 452 Doak, D.F. & Morris, W.F. (2010). Demographic compensation and tipping points in climate-induced
 453 range shifts. *Nature*, 467, 959–962.
- 454 Doak, D.F., Morris, W.F., Pfister, C., Kendall, B.E. & Bruna, E.M. (2005). Correctly Estimating How
 455 Environmental Stochasticity Influences Fitness and Population Growth. *The American Naturalist*,
 456 166, E14–E21.
- 457 Franco, M. & Silvertown, J. (2004). A comparative demography of plants based upon elasticities of vital
 458 rates. *Ecology*, 85, 531–538.
- 459 García-Camacho, R., Albert, M.J. & Escudero, A. (2012). Small-scale demographic compensation in a high-
 460 mountain endemic: the low edge stands still. *Plant Ecology & Diversity*, 5, 37–44.
- 461 Giménez-Benavides, L., Albert, M.J., Iriondo, J.M. & Escudero, A. (2011). Demographic processes of
 462 upward range contraction in a long-lived Mediterranean high mountain plant. *Ecography*, 34,
 463 85–93.

464 Hastings, A. & Botsford, L.W. (2006). Persistence of spatial populations depends on returning home.
465 *Proceedings of the National Academy of Sciences of the United States of America*, 103, 6067–
466 6072.

467 Jongejans, E., Kroon, H.D., Tuljapurkar, S. & Shea, K. (2010). Plant populations track rather than buffer
468 climate fluctuations. *Ecology Letters*, 13, 736–743.

469 Kattge, J., Díaz, S., Lavorel, S., Prentice, I.C., Leadley, P., Bönnisch, G., *et al.* (2011). TRY – a global database
470 of plant traits. *Global Change Biology*, 17, 2905–2935.

471 Kim, E. & Donohue, K. (2011). Demographic, developmental and life-history variation across altitude in
472 *Erysimum capitatum*. *J. Ecol.*, 99, 1237–1249.

473 Knops, J.M.H., Koenig, W.D. & Carmen, W.J. (2007). Negative correlation does not imply a tradeoff
474 between growth and reproduction in California oaks. *Proc Natl Acad Sci U S A*, 104, 16982–
475 16985.

476 Laiolo, P. & Obeso, J.R. (2017). Life-History Responses to the Altitudinal Gradient. In: *High Mountain*
477 *Conservation in a Changing World* (eds. Catalan, J., Ninot, J.M. & Aniz, M.M.). Springer
478 International Publishing, Cham, pp. 253–283.

479 Lande, R., Engen, S. & Saether, B.-E. (2003). *Stochastic Population Dynamics in Ecology and Conservation*.
480 Oxford University Press.

481 Lauber, K., Gerhart, W. & Gygas, A. (2018). *Flora Helvetica - Flore illustrée de Suisse*. Haupt Verlag.

482 Lewontin, R.C. & Cohen, D. (1969). On Population Growth in a Randomly Varying Environment.
483 *Proceedings of the National Academy of Sciences of the United States of America*, 62, 1056–
484 1060.

485 Meehl, G.A. & Tebaldi, C. (2004). More Intense, More Frequent, and Longer Lasting Heat Waves in the
486 21st Century. *Science*, 305, 994–997.

487 Miller, T.E.X., Louda, S.M., Rose, K.A. & Eckberg, J.O. (2009). Impacts of insect herbivory on cactus
488 population dynamics: experimental demography across an environmental gradient. *Ecological*
489 *Monographs*, 79, 155–172.

490 Moles, A.T., Perkins, S.E., Laffan, S.W., Flores-Moreno, H., Awasthy, M., Tindall, M.L., *et al.* (2014). Which
491 is a better predictor of plant traits: temperature or precipitation? *Journal of Vegetation Science*,
492 25, 1167–1180.

493 Morris, W.F., Pfister, C.A., Tuljapurkar, S., Haridas, C.V., Boggs, C.L., Boyce, M.S., *et al.* (2008). Longevity
494 Can Buffer Plant and Animal Populations Against Changing Climatic Variability. *Ecology*, 89, 19–
495 25.

496 Nakagawa, S., Johnson, P.C.D. & Schielzeth, H. (2017). The coefficient of determination R² and intra-class
497 correlation coefficient from generalized linear mixed-effects models revisited and expanded.
498 *Journal of The Royal Society Interface*, 14, 20170213.

499 Nguyen, V., Buckley, Y.M., Salguero-Gómez, R. & Wardle, G.M. (2019). Consequences of neglecting
500 cryptic life stages from demographic models. *Ecological Modelling*, 408, 108723.

501 Nobis, M.P. & Schweingruber, F.H. (2013). Adult age of vascular plant species along an elevational land-
502 use and climate gradient. *Ecography*, 36, 1076–1085.

503 Oostermeijer, J.G.B., Brugman, M.L., De Boer, E.R. & Nijs, H.C.M.D. (1996). Temporal and Spatial
504 Variation in the Demography of *Gentiana Pneumonanthe*, a Rare Perennial Herb. *Journal of*
505 *Ecology*, 84, 153–166.

506 Ouborg, N.J. & Eriksson, O. (2004). Toward a Metapopulation Concept for Plants. In: *Ecology, Genetics*
507 *and Evolution of Metapopulations* (eds. Hanski, I. & Gaggiotti, O.E.). Academic Press, Burlington,
508 pp. 447–469.

509 Pena-Gomez, F.T. & Bustamante, R.O. (2012). Life history variation and demography of the invasive plant
510 *Eschscholzia californica* Cham. (Papaveraceae), in two altitudinal extremes, Central Chile. *Gayana*
511 *Bot.*, 69, 113–122.

512 Philipp, M., Hansen, K., Monrad, D., Adersen, H., Bruun, H.H. & Nordal, I. (2018). Hidden biodiversity in
513 the Arctic – a study of soil seed banks at Disko Island, Qeqertarsuaq, West Greenland. *Nordic*
514 *Journal of Botany*, 36, e01721.

515 Pianka, E.R. (1970). On r- and K-Selection. *The American Naturalist*, 104, 592–597.

516 Pironon, S., Papuga, G., Villellas, J., Angert, A.L., García, M.B. & Thompson, J.D. (2017). Geographic
517 variation in genetic and demographic performance: new insights from an old biogeographical
518 paradigm. *Biological Reviews*, 92, 1877–1909.

519 Poloczanska, E.S., Brown, C.J., Sydeman, W.J., Kiessling, W., Schoeman, D.S., Moore, P.J., *et al.* (2013).
520 Global imprint of climate change on marine life. *Nature Climate Change*, 3, 919–925.

521 Read, Q.D., Moorhead, L.C., Swenson, N.G., Bailey, J.K. & Sanders, N.J. (2014). Convergent effects of
522 elevation on functional leaf traits within and among species. *Functional Ecology*, 28, 37–45.

523 Rosbakh, S., Römermann, C. & Poschlod, P. (2015). Specific leaf area correlates with temperature: new
524 evidence of trait variation at the population, species and community levels. *Alp Botany*, 125, 79–
525 86.

526 Salguero-Gómez, R., Jones, O.R., Jongejans, E., Blomberg, S.P., Hodgson, D.J., Mbeau-Ache, C., *et al.*
527 (2016). Fast–slow continuum and reproductive strategies structure plant life-history variation
528 worldwide. *Proceedings of the National Academy of Sciences*, 113, 230–235.

529 Schär, C., Vidale, P.L., Lüthi, D., Frei, C., Häberli, C., Liniger, M.A., *et al.* (2004). The role of increasing
530 temperature variability in European summer heatwaves. *Nature*, 427, 332–336.

531 Schinner, F., Öhlinger, R., Kandeler, E. & Margesin, R. (Eds.). (1996). *Methods in Soil Biology*. Springer-
532 Verlag, Berlin Heidelberg.

533 Sheth, S.N. & Angert, A.L. (2018). Demographic compensation does not rescue populations at a trailing
534 range edge. *PNAS*, 115, 2413–2418.

535 Silvertown, J., Franco, M. & Menges, E. (1996). Interpretation of Elasticity Matrices as an Aid to the
536 Management of Plant Populations for Conservation. *Conservation Biology*, 10, 591–597.

537 Silvertown, J., Franco, M., Pisanty, I. & Mendoza, A. (1993). Comparative Plant Demography - Relative
538 Importance of Life-Cycle Components to the Finite Rate of Increase in Woody and Herbaceous
539 Perennials. *J. Ecol.*, 81, 465–476.

540 Smith, M.D. (2011). The ecological role of climate extremes: current understanding and future prospects:
541 Ecological role of climate extremes. *Journal of Ecology*, 99, 651–655.

542 Thuiller, W., Guéguen, M., Georges, D., Bonet, R., Chalmandrier, L., Garraud, L., *et al.* (2014). Are
543 different facets of plant diversity well protected against climate and land cover changes? A test
544 study in the French Alps. *Ecography*, 37, 1254–1266.

545 Tuljapurkar, S. (1990). *Population Dynamics in Variable Environments*. Lecture Notes in Biomathematics.
546 Springer Berlin Heidelberg, Berlin, Heidelberg.

547 Tuljapurkar, S., Horvitz, C.C. & Pascarella, J.B. (2003). The many growth rates and elasticities of
548 populations in random environments. *The American Naturalist*, 162, 489–502.

549 Villellas, J., Doak, D.F., García, M.B. & Morris, W.F. (2015). Demographic compensation among
550 populations: what is it, how does it arise and what are its implications? *Ecology Letters*, 18,
551 1139–1152.

552 Villellas, J., Morris, W.F. & García, M.B. (2013). Variation in stochastic demography between and within
553 central and peripheral regions in a widespread short-lived herb. *Ecology*, 94, 1378–1388.

554 de Villemereuil, P., Mouterde, M., Gaggiotti, O.E. & Till-Bottraud, I. (2018). Patterns of phenotypic
555 plasticity and local adaptation in the wide elevation range of the alpine plant *Arabis alpina*.
556 *Journal of Ecology*, 106, 1952–1971.

557 Wang, R., Farrona, S., Vincent, C., Joecker, A., Schoof, H., Turck, F., *et al.* (2009). *PEP1* regulates perennial
558 flowering in *Arabis alpina*. *Nature*, 459, 423–427.

559 Williams, J.L., Jacquemyn, H., Ochocki, B.M., Brys, R. & Miller, T.E.X. (2015). Life history evolution under
560 climate change and its influence on the population dynamics of a long-lived plant. *Journal of*
561 *Ecology*, 103, 798–808.
562 Zuur, A., Ieno, E.N., Walker, N., Saveliev, A.A. & Smith, G.M. (2009). *Mixed Effects Models and Extensions*
563 *in Ecology with R*. Springer Science & Business Media.
564

565 **SUPPORTING INFORMATION**

566 Additional Supporting Information may be downloaded via the online version of this article at Wiley
567 Online Library (www.ecologyletters.com).

568

569 Figure legends

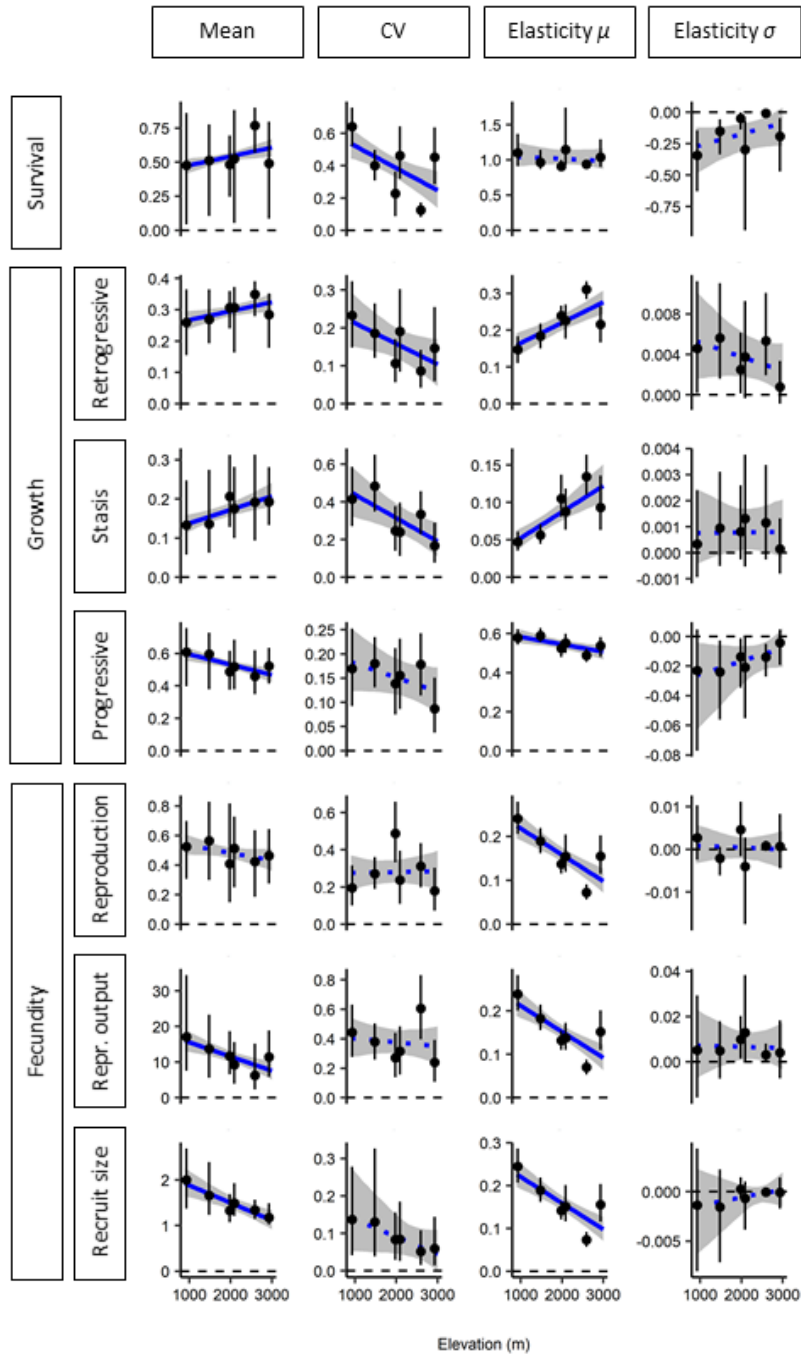
570 **Figure 1. Elevational patterns in life-cycle components and elasticities.** Elevational patterns in mean
571 life-cycle components, coefficients of variation (CV) of life-cycle components, elasticities to means (μ)
572 and elasticities to standard deviation (σ) of life-cycle components. Life-cycle components are survival (S),
573 retrogressive growth (G^-), stasis ($G^=$), progressive growth (G^+), reproduction (F_0), reproductive output (F_1)
574 and recruit size (F_2). Dots are mean values and bars extend over 95% confidence intervals. The blue lines
575 are fitted linear regressions between values and elevation, and the gray areas are 95% confidence
576 intervals. Solid lines indicate significant regressions ($p < 0.05$). Confidence intervals and significance
577 values were calculated by randomly sampling statistical models over 200 bootstrapped demographic
578 datasets and 10 resampled imputed climatic datasets

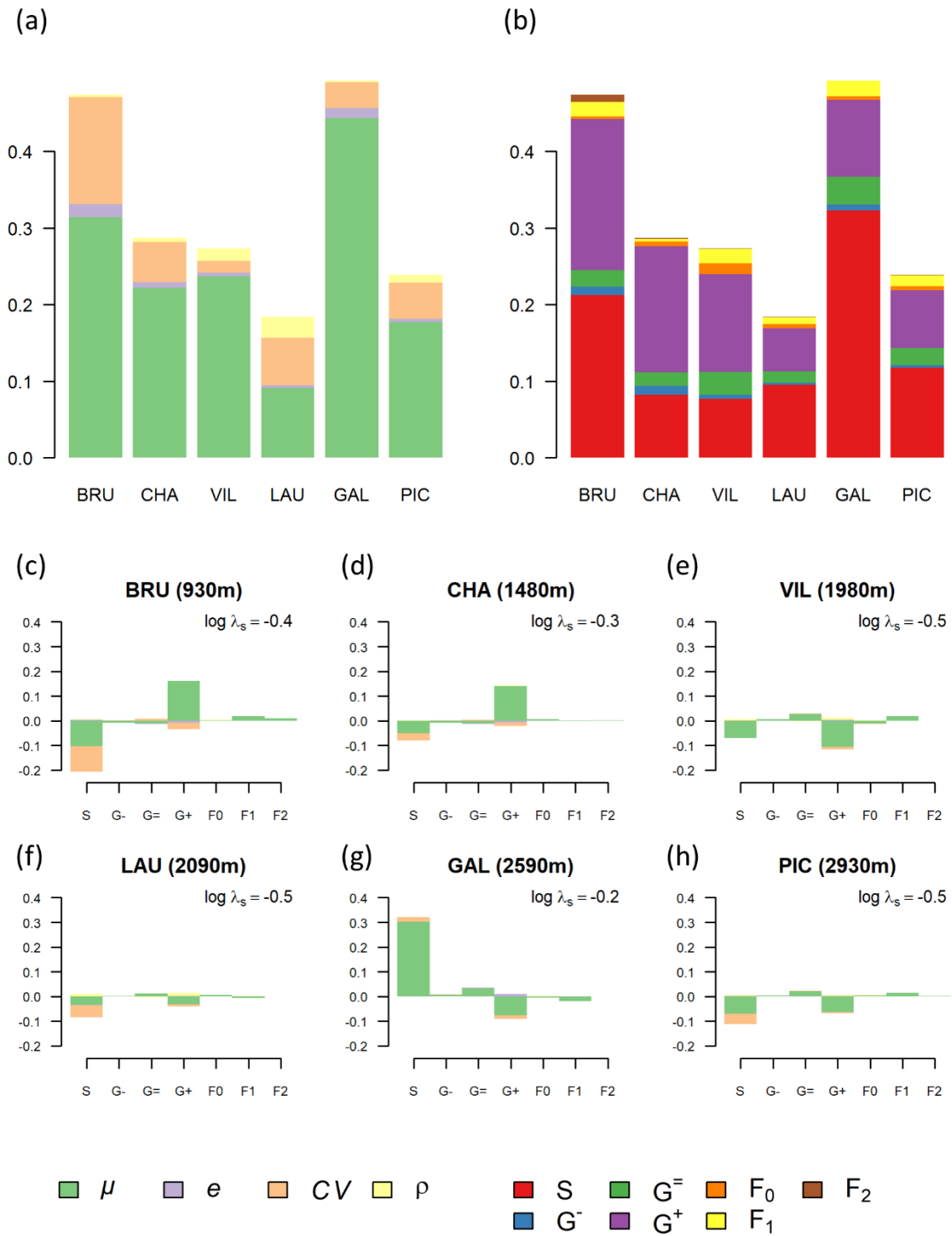
579 **Figure 2. Stochastic life-table response experiment (SLTRE).** Total effects of each descriptor (a) and life-
580 cycle component (b) to differences in stochastic population growth rates ($\log\lambda_s$) between the focal site
581 and a reference site constructed by taking the mean of vital rates over all sites. (c) to (h), net
582 contributions C_l^k of each descriptor k of each life-cycle component l to the difference in $\log\lambda_s$. Negative
583 and positive contributions are plotted separately. Colours indicate the descriptor (μ , means; e ,
584 elasticities; CV , coefficients of variation; ρ , temporal correlations) or the life-cycle component (S,
585 survival; G^- , retrogressive growth; $G^=$, stasis; G^+ , progressive growth; F_0 , reproduction; F_1 , fecundity; F_2 ,
586 recruit size).

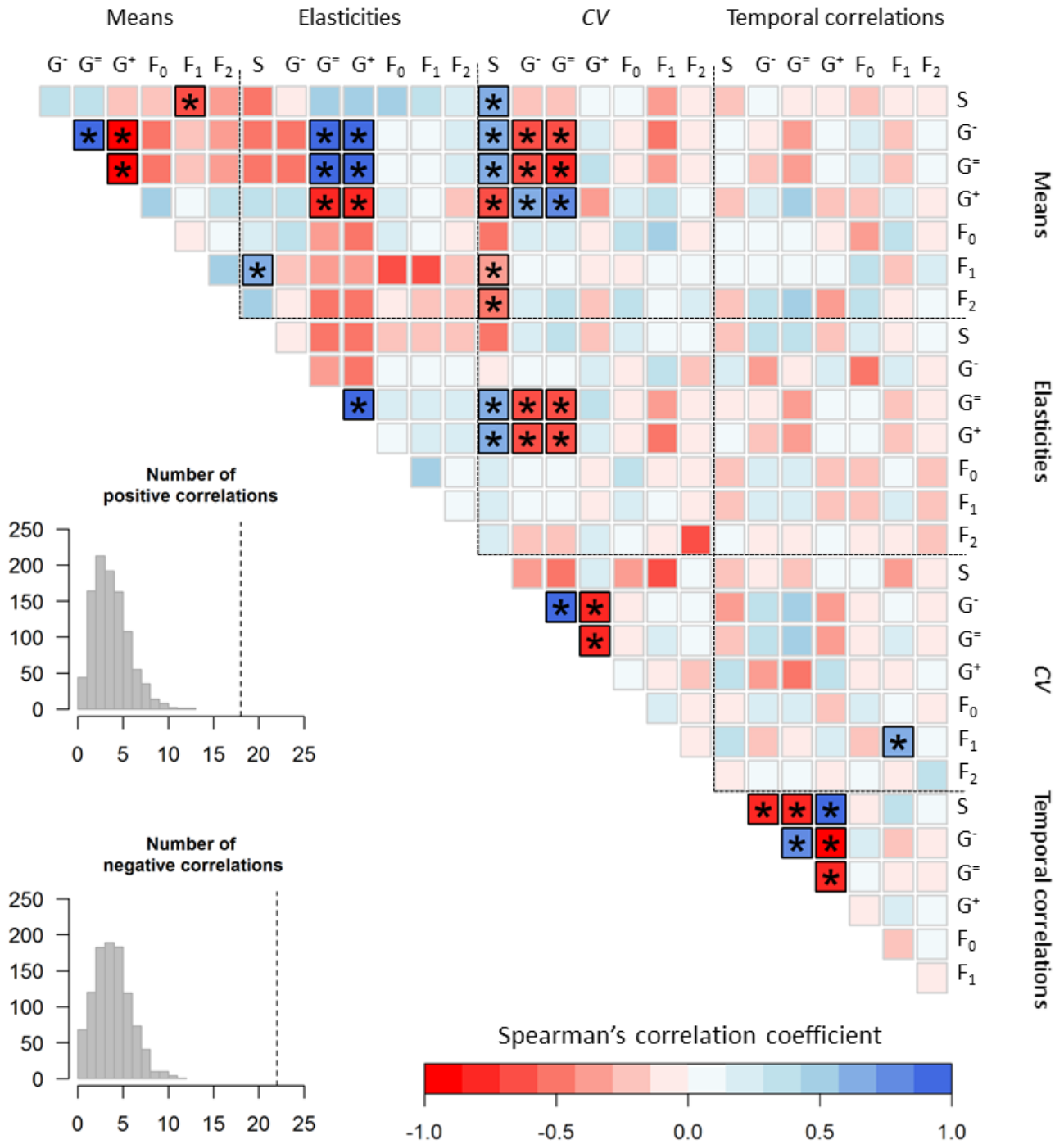
587 **Figure 3. Demographic compensation.** Correlogram of Spearman's correlation coefficients between the
588 net contributions of different descriptors of life-cycle components to differences in stochastic population
589 growth rates ($\log\lambda_s$) between sites (SLTRE contributions). Negative correlations are in red, positive
590 correlations are in blue. Boxes with thicker borders and an asterisk indicate significant correlations at $p <$
591 0.05. The insets show the number of observed significant positive and negative correlations (vertical

592 dotted lines) compared to the distribution of the number expected by chance obtained through a
593 permutation test (histograms). See Figure 2 for definitions of descriptors and life-cycle components.

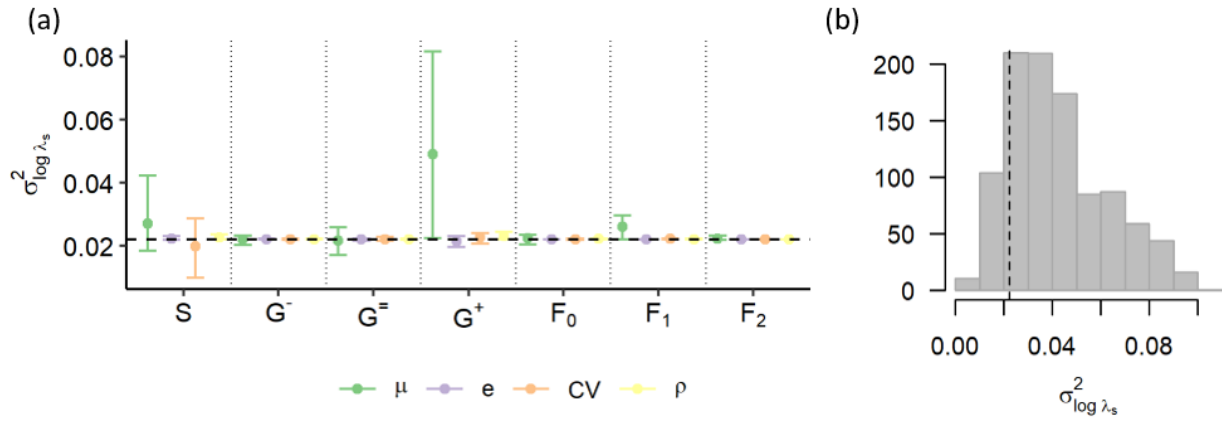
594 **Figure 4. Effectiveness of demographic compensation.** (a), variance of population growth rate $\log\lambda_s$
595 between sites, $\sigma_{\log\lambda_s}^2$, obtained by permuting each descriptor of each life-cycle component at a time.
596 Dots are mean values and bars extend over 95% confidence intervals over 1000 permutations. Values
597 higher than the observed $\sigma_{\log\lambda_s}^2$ (horizontal dashed line) indicate that the corresponding parameter
598 effectively reduces $\sigma_{\log\lambda_s}^2$ through demographic compensation. (b), observed $\sigma_{\log\lambda_s}^2$ (vertical dotted
599 lines) compared to the distribution of $\sigma_{\log\lambda_s}^2$ expected by chance obtained through permuting only the
600 parameters effectively reducing it (histograms). See Figure 2 for definitions of descriptors and life-cycle
601 components.







608 **FIGURE 4**



609

Table 1. Characteristics of the study sites.

Site	BRU	CHA	VIL	LAU	GAL	PIC
Longitude	5.61112	5.59267	5.57083	6.39034	6.40375	6.38426
Latitude	45.15065	45.07117	45.01809	45.02846	45.06049	45.06385
Elevation (m)	930	1480	1980	2090	2590	2930
Aspect	South	North	South	North	North	South
Habitat	Calcareous scree	Calcareous grassland, scree	Calcareous scree	Schists, torrent	Calcareous scree	Schistose scree
Initial N	46	145	104	90	110	50
Number of plots	2	3	3	3	3	4
T_{mean}	14.7 (12.8, 17.5)	15.7 (12.9, 18.2)	12.9 (9.3, 17.5)	10.4 (8.0, 12.1)	7.7 (5.3, 10.3)	9.1 (5.9, 12.1)
T_{range}	11 (6.0, 18.6)	16.9 (11.5, 21.9)	15.9 (9.7, 36.1)	6.3 (3.1, 9.6)	8.1 (5.8, 13.3)	16.3 (11.8, 23.2)
$\log\lambda_s$	-0.4 (-0.5, -0.2)	-0.3 (-0.5, -0.2)	-0.5 (-0.6, -0.4)	-0.5 (-0.8, -0.3)	-0.2 (-0.2, -0.1)	-0.5 (-0.8, -0.3)

N , number of individuals. Daily mean temperature (T_{mean}) and daily temperature range (T_{range}) were measured with *in-situ* data-loggers. Values are means and (minimum and maximum) over plots and years for the month of July. Means and 95% confidence interval for the stochastic population growth rate ($\log\lambda_s$) were calculated by randomly sampling the values calculated using matrix populations models constructed using predicted vital rates from 200 bootstrapped demographic datasets and 10 resampled imputed datasets. The N per site per year is shown in

Figure S2.

Table 2. Statistical analysis of plant vital rates.

Predictor	Survival		Growth		Reproduction		Reproductive output		Recruit size	
	mean	95% CI	mean	95% CI	mean	95% CI	mean	95% CI	mean	95% CI
Fixed effects										
Intercept	0.50	(0.31, 0.72)	1.35	(1.24, 1.44)	0.75	(0.35, 1.26)	1.05	(0.99, 1.10)	-0.76	(-1.11, -0.50)
<i>SoilVeg</i> ₁	-0.27	(-0.69, 0.19)	0.17	(-0.18, 0.35)	0.10	(-0.36, 0.77)	0.03	(-0.06, 0.15)	0.57	(-0.16, 1.07)
<i>SoilVeg</i> ₂	-0.29	(-0.77, 0.05)	0.17	(0.03, 0.38)	0.14	(-0.26, 0.69)	0.10	(0.01, 0.18)	-0.04	(-0.80, 0.49)
Plant size	0.79	(0.47, 1.09)	1.26	(1.09, 1.43)	3.78	(3.04, 4.61)	0.58	(0.49, 0.69)	-	-
(Plant size) ²	-0.56	(-0.88, -0.3)	-0.71	(-0.87, -0.57)	-1.37	(-2.21, -0.74)	-0.26	(-0.37, -0.18)	-	-
<i>T</i> _{mean}	-3.52	(-5.08, 0.22)	0.35	(-0.24, 1.75)	0.04	(-2.34, 2.53)	-0.06	(-0.58, 0.41)	0.55	(-2.47, 3.33)
(<i>T</i> _{mean}) ²	3.37	(0.17, 5.04)	-0.51	(-1.76, 0.16)	-0.13	(-2.66, 2.24)	-0.02	(-0.42, 0.52)	0.52	(-2.67, 3.20)
<i>T</i> _{range}	-0.40	(-0.95, 0.05)	0.01	(-0.23, 0.25)	0.33	(-0.10, 1.19)	0.11	(0.00, 0.20)	-0.63	(-1.78, -0.07)
Random effects										
Site (Intercept)	0.00	(0.00, 0.55)	0.08	(0.00, 0.55)	0.00	(0.00, 0.72)	0.12	(0.00, 0.23)	0.00	(0.00, 0.40)
Year (Intercept)	0.51	(0.22, 0.86)	0.41	(0.33, 0.50)	1.09	(0.84, 1.40)	0.15	(0.11, 0.19)	0.00	(0.00, 0.70)
Year (<i>SoilVeg</i> ₂)	1.27	(0.82, 1.83)	-	-	-	-	-	-	-	-
Year (Intercept * <i>SoilVeg</i> ₂)	0.15	(-0.48, 0.98)	-	-	-	-	-	-	-	-
Plot (Intercept)	-	-	-	-	1.28	(0.87, 1.88)	-	-	-	-
Plot (Plant size)	-	-	-	-	1.52	(0.85, 2.56)	-	-	-	-
Plot (Intercept * Plant size)	-	-	-	-	0.95	(0.74, 1.00)	-	-	-	-
Residual	-	-	1.62	(1.39, 1.89)	-	-	0.36	(0.34, 0.38)	2.61	(0.86, 13436)
Marginal <i>R</i> ²	0.07	(0.03, 0.12)	0.25	(0.2, 0.31)	0.46	(0.38, 0.56)	0.44	(0.36, 0.53)	0.04	(0.00, 0.10)
Conditional <i>R</i> ²	0.41	(0.29, 0.56)	0.36	(0.3, 0.49)	0.80	(0.69, 0.88)	0.57	(0.51, 0.64)	0.05	(0.02, 0.18)

For each of the five vital rates, the table reports the standardized coefficients of fixed effect, the standard deviation of random effects (intercepts and slopes), the correlations between random intercept and slopes and marginal and conditional R^2 (Nakagawa *et al.* 2017). Only the random effects that were retained after model selection on the random structure are shown. Means and 95% confidence intervals were calculated by randomly sampling statistical models over 200 bootstrapped demographic datasets and 10 resampled imputed datasets. The predictors whose confidence intervals do not overlap with zero are in **bold**.